Construction and Building Materials 492 (2025) 142819

Contents lists available at ScienceDirect

Construction and Building Materials

journal homepage: www.elsevier.com/locate/conbuildmat

An integrated packing-moisture control approach in bitumen-stabilized materials (BSM) design

Sajjad Noura [a,*], Andrea Graziani [b], Alan Carter [a]

[a] Construction engineering department, École de technologie supérieure (ÉTS), 1100, Notre-Dame Street West, Montréal, Canada
[b] Department of Civil and Building Engineering, and Architecture, Università Politecnica delle Marche, Via Brecce Bianche, Ancona 60131, Italy

ARTICLE INFO

Keywords:
Cold recycled mixtures
Bitumen-stabilized materials
Reclaimed asphalt pavement
Aggregate packing
Voids filled with liquid control
Volumetric mix design

ABSTRACT

The mechanical performance of bitumen-stabilized materials (BSM) hinges on two interrelated factors, including aggregate packing and moisture control. However, current design practices offer little guidance on how to systematically balance these variables. This study, therefore, proposes an integrated volumetric framework that couples the Bailey packing principles with a liquid-filled-voids (VFL) criterion to identify the optimum aggregate gradation and total water content for mixtures composed entirely of reclaimed asphalt pavement (RAP). Four gradations were manufactured by blending coarse and fine RAP to represent 60 %, 80 %, 90 %, and 100 % of their loose-unit-weight (LUW) packing states. Each blend was stabilized with a 3 % residual bitumen emulsion and total water dosages ranging from 3 % to 6 %. Compaction behaviour was captured through the dry density, voids filled with liquid (VFL), and voids in the mixture (V_m), which were monitored for up to 100 gyrations. In contrast, water loss due to compaction, long-term evaporation, and 56-day indirect tensile strength (ITS) were also assessed. Results indicate that the 80LUW gradation, combined with a total water dosage of 4 %-4.5 %, produced the densest internal structure ($V_m \approx 8.4$ %) and maintained VFL at the 85 % threshold that prevents liquid seepage. In contrast, finer (60 %LUW) and coarser (90–100 %LUW) gradations exhibited excessive voids at comparable moisture levels. The proposed framework thus offers a practical way for selecting gradation–moisture combinations, reducing experimental repetition and advancing the sustainable use of BSMs.

1. Introduction

Sustainability in road construction is a critical subject that focuses on solutions to problems associated with recyclability, waste products, environmental pollution, and the scarcity of virgin materials, among others [1,2]. One of the most important recyclable materials in road construction is reclaimed asphalt pavement (RAP), which is used in hot mix asphalt (HMA) for rehabilitation purposes. However, a more environmentally friendly application of RAP is in cold pavement recycling [3,4]. Cold recycling technologies include full-depth reclamation (FDR) and cold recycled mixtures (CRM), which include cold in-place recycling (CIR) and cold central plant recycling (CCPR) [1,5]. Due to their cost-effectiveness and environmentally friendly application, which utilizes up to 100 % of the reclaimed asphalt pavement (RAP), these processes are considered attractive sustainability methods. These methods include milling of overlay and/or the base materials, and recycling the asphalt pavement with cold techniques without heat application [1,6].

Due to their low production temperature and the reduction in the use of virgin aggregate, which utilizes over 85 % of RAP, CRM has received considerable attention. There are several types of CRM, including cement-treated materials (CTM), bitumen-stabilized materials (BSM), cold recycled asphalt (CRA), and cement-bitumen-treated materials (CBTM), which are treated with both bitumen emulsion and foamed bitumen. When compared to CBTM, BSM uses less cement (less than 1 %) [7,8]. Due to the inclusion of water in the CRM design, they will require a curing time to lose water and gain strength over time, a process also referred to as evolutive behaviour, which affects their evolutive behaviour over time. Hydraulic binders act as an agent that accelerates the curing process [9,10].

The most important components of BSM with emulsion include RAP, water, and bitumen emulsion (with residual bitumen more than 1.5 % and less than 3 %). Still, small amounts of active fillers (less than 2 %) may be added to accelerate the curing time [8,11,2,12,13]. Limiting the amount of cement helps reduce the rigidity, and adding bitumen content increases BSM's flexibility.

BSM may include granular materials, cement stabilized materials,

* Corresponding author.
E-mail address: Sajjad.noura.1@ens.etsmtl.ca (S. Noura).

https://doi.org/10.1016/j.conbuildmat.2025.142819
Received 28 May 2025; Received in revised form 9 July 2025; Accepted 19 July 2025
Available online 5 August 2025

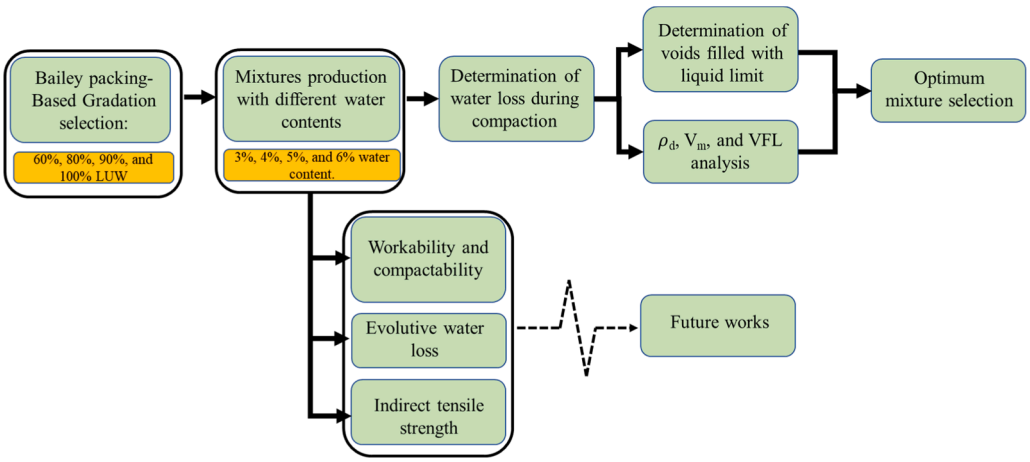

Fig. 1. Flowchart of the methodology.

Table 1
Coarse and Fine RAP properties.

Property	Value	Specification
Coarse RAP relative specific gravity, g/cm3	2.514	ASTM C127–24
Fine RAP relative specific gravity, g/cm3	2.296	ASTM C128–22
Coarse RAP relative SSD density, g/cm3	2.549	ASTM C127–24
Fine RAP relative SSD density, g/cm3	2.338	ASTM C128–22
Coarse RAP absorption, %	1.399	ASTM C127–24
Fine RAP absorption, %	1.825	ASTM C128–22
Flat coarse particles, %	13.73	ASTM D4791
Elongated coarse particles, %	10.80	ASTM D4791
Flat and elongated coarse particles, %	1.53	ASTM D4791

Table 2
Bitumen emulsion properties.

Property	Value	Specification	Min.	Max.
Type of bitumen emulsion	CSS−1	ASTM 7402	N/A	N/A
Passing 850 μm, % mass	0.02	ASTM D6933	N/A	0.1
Distillation residue at 260 °C, %	65.1	ASTM D6997	57	N/A
Saybolt Furol viscosity at 25 °C, s	36.7	ASTM D7496	20	100
Oil in the distillation, %	0.2	ASTM D6997	N/A	5
Penetration at 25 °C	168	ASTM D5	100	250

Fig. 2. (a) Rodded Coarse RAP; (b) Rodded Fine RAP.

and RAP, which makes them suitable for both new pavement constructions and the rehabilitation of in-place and central plants [14]. They also offer enhanced properties of recycled materials at reduced costs. Asphalt Academy (2020) explained that the failure mode in BSM is permanent deformation and that the pavement will require less effort to rehabilitate than a material that fails due to full-depth cracking, and that the changes in behaviour can be changed by the quantity of the bitumen and cement content [15].

Table 3
Bailey unit weights and voids for coarse and fine RAP.

Property	Value
Coarse RAP LUW, kg/m3	1355.62
Fine RAP LUW, kg/m3	1347.52
Coarse RAP RUW, kg/m3	1491.91
Fine RAP RUW, kg/m3	1489.68
Coarse RAP Solid unit weight (SUW), kg/m3	2514.0
Fine RAP Solid unit weight (SUW), kg/m3	2310
Coarse aggregate loose voids, %	46.08
Fine aggregate loose voids, %	41.66
Coarse aggregate rodded voids, %	40.66
Fine aggregate rodded voids, %	35.51

Generally, packing characteristics and air void reductions are among the most important factors influencing the mechanical properties and performance of asphalt mixtures, including permanent deformation and damage during freeze-thaw cycles [16,17]. It is known that an improvement in the packing helps with a reduction in permanent deformation [18]. Badeli et al. [17] experimentally explained that air voids also have a significant influence on complex modulus behaviour when the specimens are subjected to freeze-thaw cycles.

Aggregate packing is influenced by five factors: aggregate gradation, aggregate strength, aggregate morphological properties (shape, angularity, aggregate surface micro-texture), compaction method, and compaction effort [19–22]. Although researchers have been attempting to identify best practices for CRM, particularly for BSM mixtures, there is no uniform mix design procedure for these materials. Different agencies, including AASHTO, ARRA, and Asphalt Academy, have suggested gradation boundaries for BSM mixtures [23–27]. Many studies attempted various methods to evaluate compaction, volumetrics, and performance of CRM by changing the gradation of CRM [13,19,20,28,29–34]. Xu et al. (2017) investigated the aggregate fractal analysis of three CRM gradations to determine how gradation and binder content impact mixture performance. They suggested using fractal dimensions to characterize mineral aggregate fractions [19]. Raschia et al. (2021) employed the compressible packing model to investigate how RAP sources impact the virtual packing densities of RAP aggregate blends and the compactability of CRM mixtures [20]. Yao et al. (2011) mentioned using the Bailey method to optimize the gradations and mechanical properties of CRM manufactured using 70 % RAP, with the addition of 2 % and 3 % cement, as per the Marshall method [34]. Aker and Ozer (2023) investigated the packing characteristics of CRM using the Bailey method. They evaluated discrete packing models, including Aim and Goff's, the modified Toufar model, and Kwan's 3-Parameter Packing Model, to determine the virtual packing densities and

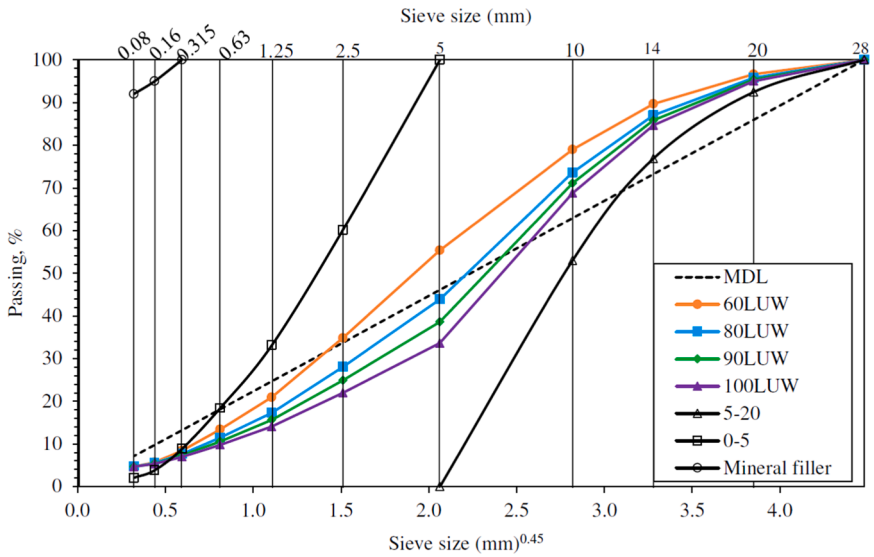

Fig. 3. Gradation curves for MDL, 60LUW, 80LUW, 90LUW, and 100LUW.

Table 4
The components of BSM mixtures are produced at different percentages of LUW based on the mass of dry solids.

Component	60LUW	80LUW	90LUW	100LUW
Coarse RAP, %	44.66	56.16	61.4	66.39
Fine RAP, %	51.40	39.67	34.29	29.20
Mineral filler, %	3.93	4.19	4.3	4.42
Absorbed water, %	1.63	1.58	1.55	1.53
Emulsion, %	4.64	4.61	4.61	4.61
Total water content, %	3.00	3.00	3.00	3.00
(±0.20 %)	4.00	4.00	4.00	4.00
	5.00	5.00	5.00	5.00
	6.00	6.00	6.00	6.00

compactability of the CRM blends [23]. Xu et al. (2017) reported that increasing the fractal value increased the passing sieve size, which was less than 0.3 mm. Mechanical performance was linked to the fineness modulus and fractal gradation dimensions. High-temperature susceptibility was affected by binder gradation and adhesion, while indirect tensile strength and moisture susceptibility were affected by gradation, bitumen emulsion content, and cement content. The balance between fractal dimension, density, and adhesion was found to be necessary for a high-performance mixture [19]. Raschia et al. (2021) investigated the workability, compactability, and mechanical properties of CRM with three gradations in Canada and Italy. They found that higher filler led to improved workability but lower compactability. Additionally, their ITS test results highlighted the significance of gradations in influencing the behaviour of CRM, with the gradation closer to the MDL proving more potent than the rest; however, adjusting the moisture content in conjunction with gradations is crucial for achieving homogeneity within the mixtures [30]. Raschia et al. (2021) found that two gradations near the MDL using 0/2.5–2.5/5–5/10 fractions were compacted at 20 gyrations. Their results showed that the two gradations used in their research had a close compactability of 83 % and 82 % at the end of compaction, and that the maximum densities could not be achieved using the model. However, their image analysis experiment using the Occhio belt aggregate image analyzer showed no significant difference in RAP shape between the two sources. Still, the RAP with a higher shape factor was more compact [20]. Yao et al. (2011) found that optimizing gradation using the Bailey method is suitable for both volumetric and mechanical properties, including determining the optimum emulsified asphalt content and the optimum water content resilient modulus [34]. Aker and Ozer (2023) utilized two coarse and two fine RAP fractions to evaluate volumetric and mechanical properties, as well as the feasibility of optimizing CRM mixtures using volumetric proportioning. Their two mixtures were shown to reach the lowest air voids of almost 12.6 % and the highest indirect tensile strength (ITS) for both 80 % LUW and 70 %

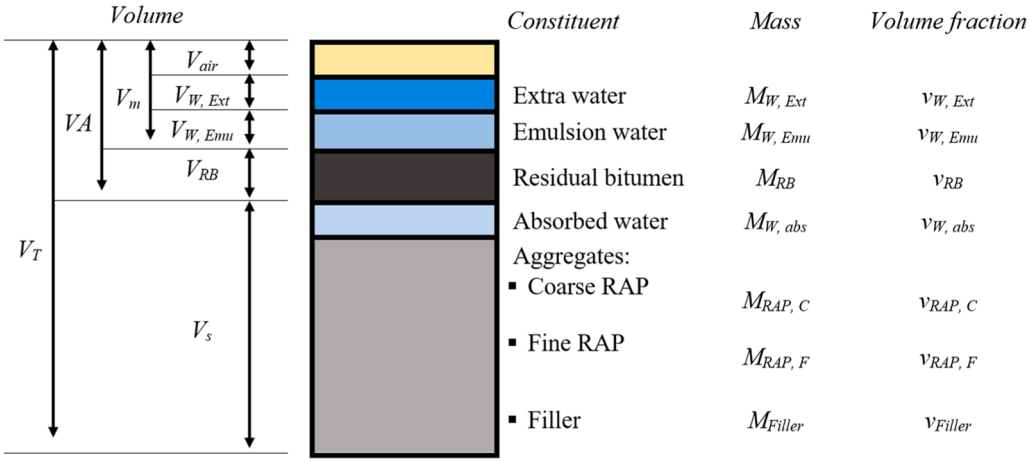

Fig. 4. Constituent materials and volumetric characteristics of BSMs.

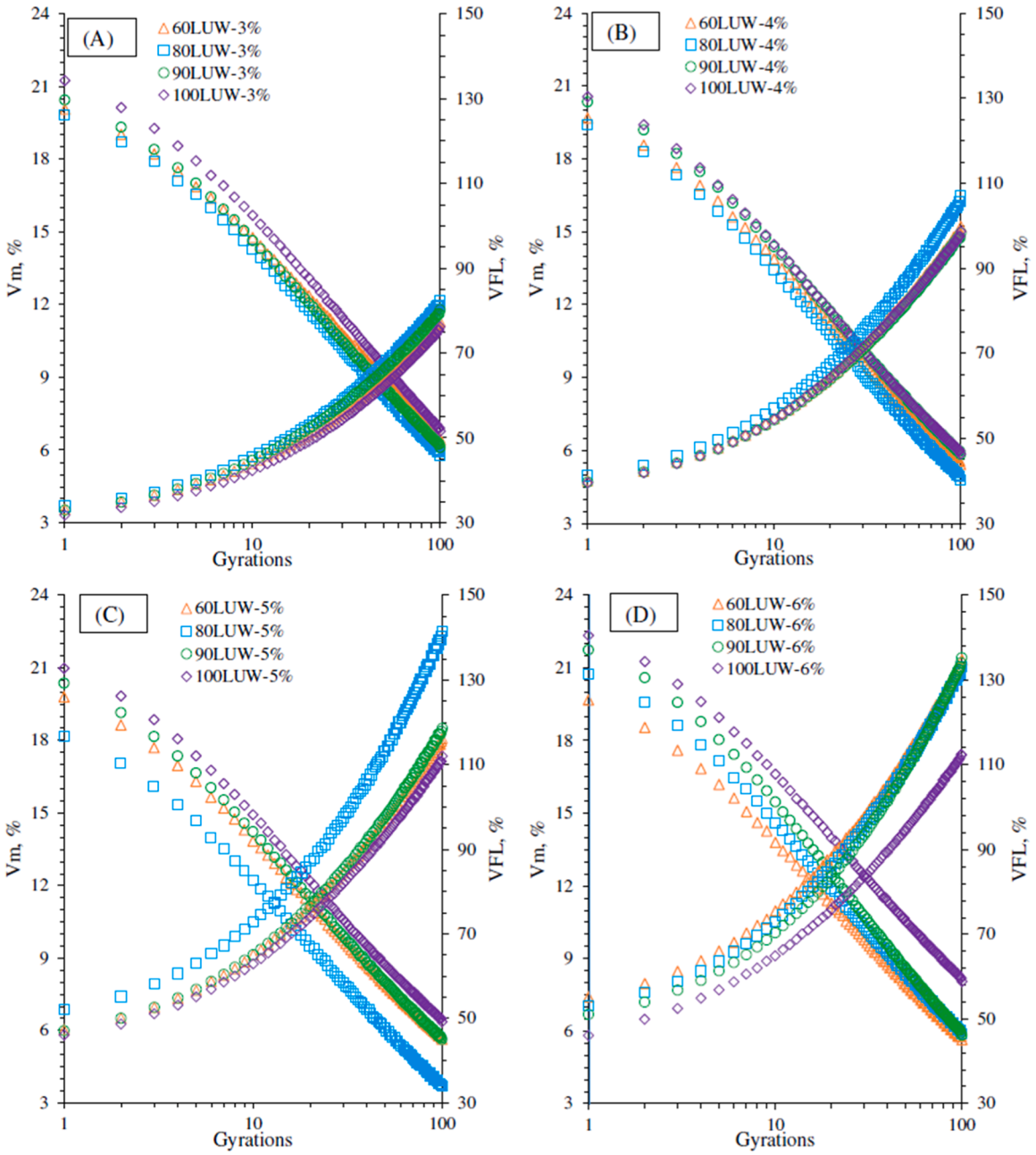

Fig. 5. V_m and VFL for different Bailey gradations at 3 % moisture content (A), 4 % moisture content (B), 5 % moisture content (C), and 6 % moisture content (D).

LUW [23].

Even though the literature suggests that by changing gradations, the mechanical properties of different types of CRM changes and some gradations could potentially improve the properties and performance of CRM, there are currently limited studies on applying a packing-moisture control approach for volumetric optimization of BSM and no study has yet studied aggregate packing of BSM with controlled water content. This paper aims to improve the mix design procedure by optimizing two aspects of gradation using the Bailey method and controlling water content using the voids filled with liquid.

2. Objectives

To address the absence of a packing-oriented procedure for the mix design of bitumen-stabilized materials (BSM), this study proposes a framework based on the Bailey method and voids filled with liquid (VFL). The procedure involves a mix design procedure that (i) identifies the aggregate gradation yielding the minimum voids in the mixtures and (ii) determines the water content required to achieve the target mixture saturation in terms of VFL. The complete methodological workflow is illustrated in Fig. 1.

3. Materials and methodology

3.1. Materials

In this study, a single-sourced RAP with a nominal maximum aggregate size (NMAS) of 20 mm was sourced from the province of Quebec, Canada. Fig. 3 shows the coarse RAP, fine RAP, and mineral filler gradations, and Table 1 shows the properties of the acquired RAP. The acquired RAP was separated into coarse and fine fractions using a 5 mm sieve. It is important to clarify that no virgin aggregate was used in this study. The bitumen emulsion used in the study was a cationic, slow-setting type designed for cold recycling applications, with the properties

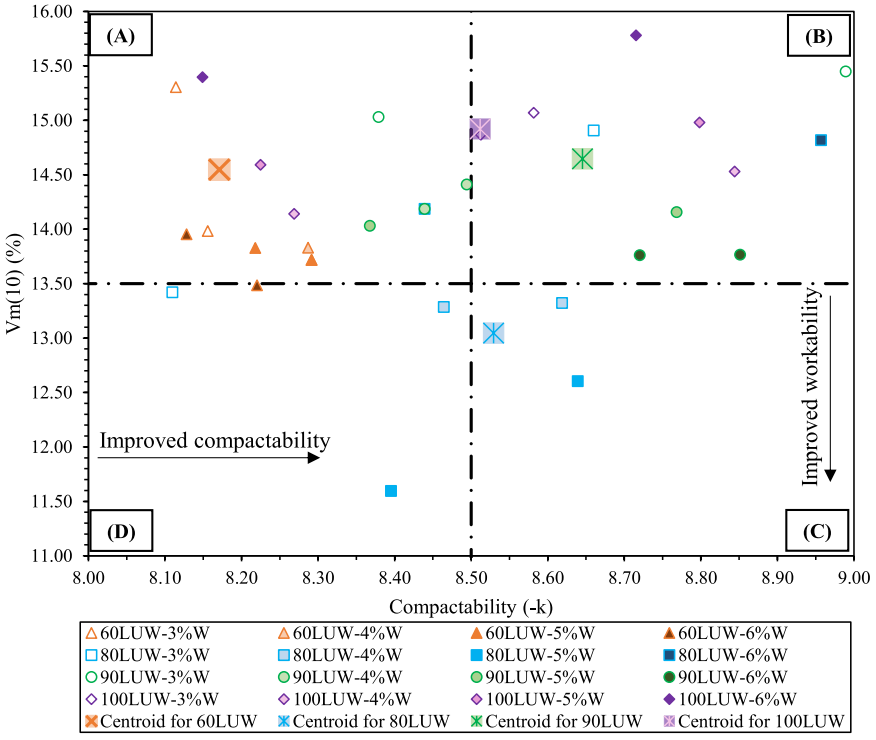

Fig. 6. Workability and compactability of the mixtures.

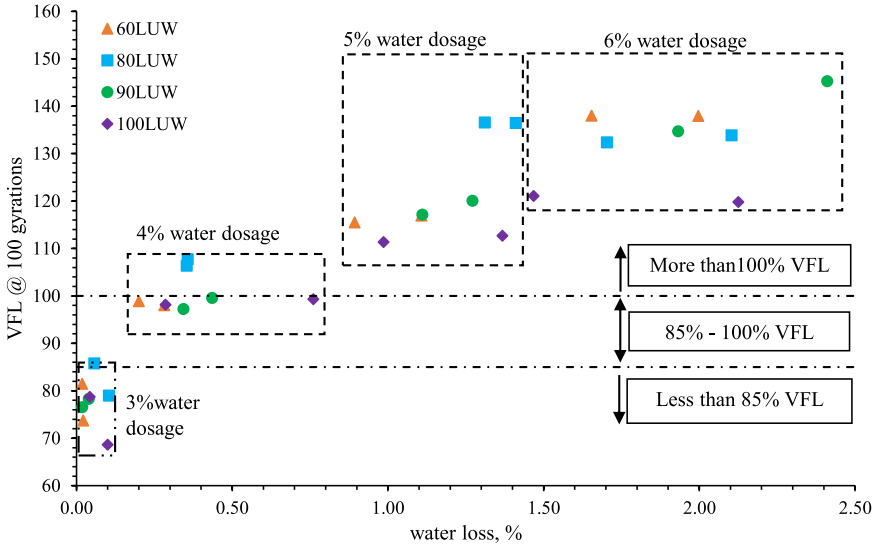

Fig. 7. VFL at 100 gyrations as a function of water loss due to compaction at the end of compaction.

shown in Table 2.

3.2. Packing-based gradation selection

The Bailey method is well-known for its packing and interlocking characteristics in reducing voids and optimizing HMA mixtures [35]. However, its application is limited to HMA mixtures containing less than 40 % of RAP. In this study, the Bailey method was employed as a packing tool for interlocking and to control the packing of coarse and fine RAP by adjusting the ratios of coarse RAP, fine RAP, and filler in the mixtures to achieve the densest possible mixture. As shown in Eq. (1), the primary control sieve (PCS) was applied in this study according to the Bailey method.

$$PCS = 0.22 * NMAS \quad (1)$$

The loose unit weight (LUW), rodded unit weight (RUW), and solid unit weight of both the coarse and fine RAP were determined on dried material at 40°C according to AASHTO T-19 and the Bailey requirements using 7.1- and 0.94-litre moulds, respectively. For LUW, the coarse and fine RAP were poured into their specific moulds without any compaction effort using the shovelling procedure. For RUW, the materials were poured in three layers in their specific moulds and rodded 25 times per layer. The loose voids and rodded voids in coarse and fine RAP were calculated according to Eqs. (5) and (6). Fig. 2 shows the rodded coarse RAP and the rodded fine RAP.

Rodded and loose voids represent the proportion of void space within

Fig. 8. (a) The seepage of water from the top of the mould due to over-saturation; (b) The seepage of water from the bottom of the mould due to over-saturation.

rodded and uncompacted (loose) conditions, respectively. According to the Bailey method, the recommended rodded voids for coarse aggregate range from 37 % to 43 %, whereas loose voids should typically fall between 43 % and 49 %. For fine particles, the Bailey method suggests rodded voids within a range of 28–36 % and loose voids from 35 % to 43 %.

Table 3 specifies the Bailey unit weights and voids for coarse and fine RAP.

$$\text{Loose Voids} = 100 * (1 - \text{Loose unit weight/Solid unit weight}) \quad (5)$$

$$\text{Rodded Voids} = 100 * (1 - \text{Rodded unit weight/Solid unit weight}) \quad (6)$$

Based on the Bailey method, it is necessary to assess a broad spectrum of packing states to obtain the theoretical maximum packing, equivalent to the highest dry density and the lowest V_m. The 60 %, 80 %, 90 %, and 100 % LUW blends were selected and will be referred to as 60LUW, 80LUW, 90LUW, and 100LUW, respectively, in this paper. Fig. 3 shows the gradation curves for 60LUW, 80LUW, 90LUW, and 100LUW.

3.3. Specimen preparation

Table 4 presents the components of BSM mixtures prepared using 60, 80, 90, and 100LUW aggregate blends. Coarse and fine RAP batches were dried at 40 °C to manufacture the mixtures. Then, a water dosage corresponding to the total absorption ratio of the coarse and fine RAP, as specified in Table 4, was added to the blends. The moist blends were kept in a sealed bag for at least 12 h to reach moisture equilibrium. To initiate the mixing process using a mechanical mixer, four water dosages were used for mixture preparation, including 3 %, 4 %, 5 %, and 6 % total water dosages. The extra water was introduced and blended thoroughly for 1 min with the pre-moistened aggregate blends to achieve the desired moisture content. Subsequently, the bitumen emulsion was incorporated into the mix and blended for 1 min to ensure uniform dispersion and coating of the particles. The compaction procedure was conducted using a Superpave gyratory compactor (SGC) at an external angle of 1.25°, a pressure of 600 ± 18 kPa, and a gyration rate of 30 rpm, as specified in ASTM D6925. For the compaction process, 2800 g of the prepared mixture was placed into a 150 mm mould and compacted at a temperature of 23 ± 2 °C and 40 % ± 15 % laboratory relative humidity. The compaction process continued up to 100 gyrations, with the specimen height measured continuously.

3.4. Volumetric analysis

Grilli et al. [24] proposed extending the volumetric analysis framework for HMA to CRM, introducing parameters such as VFL and V_m. In the context of BSM, VFL represents the volume of water and bitumen emulsion as a percentage of VMA and represents the saturation level in the mixtures; VMA refers to the total amount of voids in the skeleton which is occupied by air, total water dosage, and residual bitumen; V_m denotes the volume of air and the intergranular water content in the mixture and serves as an essential parameter for the prediction of mechanical properties of BSM during their service life. Fig. 4 illustrates the constituent parts, volume fractions, and related masses.

Eqs. (7) to (10) were utilized in this study to determine dry density, maximum density, V_m, VMA, and VFL.

$$V_m = \frac{V_{air} + V_{w,EXT} + V_{W,Emu}}{V_T} * 100 \quad (9)$$

$$VFL = \frac{V_{W,EXT} + V_{W,Emu} + V_{RB}}{V_A} * 100 \quad (10)$$

Where V_{air} is the volume of air, $V_{W,\ EXT}$ is the volume of external water (intergranular water) in the mixture, $V_{W,\ Emu}$ is the volume of water in the bitumen emulsion, V_{RB} is the volume of residual bitumen, VA is the volume of voids in mineral aggregate, and V_T is the total volume of the mixtures.

3.5. Weight loss due to compaction

During compaction, and as the specimen approaches saturation, water containing both filler particles and bitumen emulsion is squeezed out of the specimens if the mixtures approach the saturation level. Still, due to the limitations in quantifying the non-water components, it is assumed that only water is lost, and the subsequent calculations are based on this assumption. The determination of water loss due to compaction was performed by weighing the specimens immediately after compaction and the weight of the mixture right before compaction (2800 g). The water loss due to compaction is calculated using the Eq. (11):

$$\Delta W_{B,A} = \frac{W_B - W_A}{W_B} \quad (11)$$

Where $\Delta W_{B,A}$The water loss due to compaction is represented by WB, which is the weight of the mixture before compaction, and WA is the weight of the mixture after compaction.

3.6. Workability and compactability

BSM's Workability and compactability are calculated through V_m (10) and k, respectively. Compactability is the slope of compaction after 10 gyrations. It was previously reported that after 10 gyrations, the compaction curves tend to be linear in a semi-log graph [24]. The following formula is applicable when studying workability and compactability.

$$V_m(n) = V_m(10) + k * \log(n) \quad (12)$$

3.7. Curing, water loss by evaporation, and evaporation modelling

The water loss due to evaporation was monitored from 1 to 56 days after the initial mixture production, during the curing process. After the

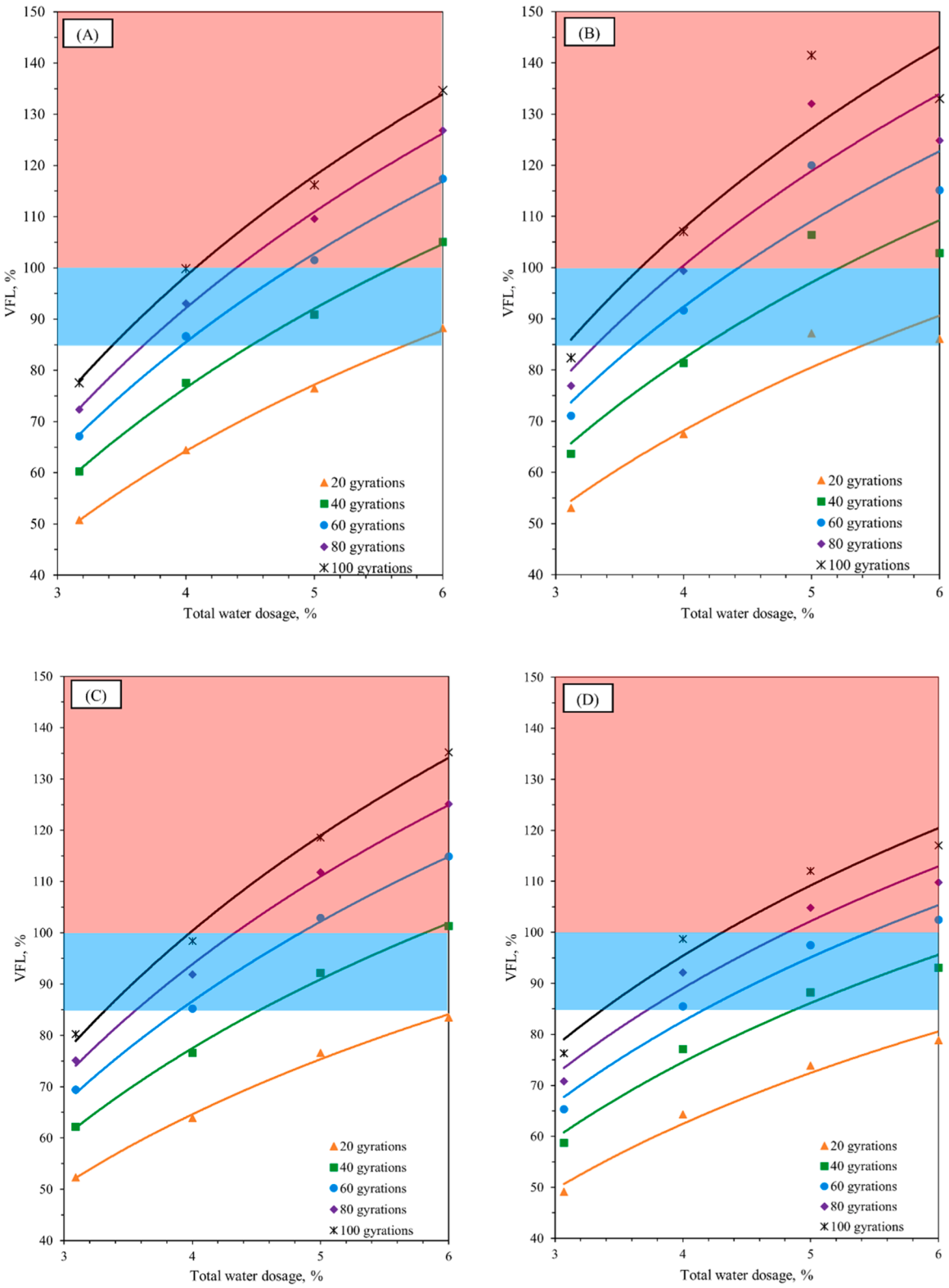

Fig. 9. VFL% as a function of total water dosage for (A): 60LUW, (B): 80LUW, (C): 90LUW, and (D): 100LUW.

mixture production, the specimens were subjected to free surface evaporation at a laboratory temperature of 23 ± 2 °C and a relative humidity of 40 % ± 15 %. Eq. (13) shows the incremental normalized water loss due to evaporation at each interval.

$$NWL_{(t)} = 100 * \frac{W_0 - W_{(t)}}{W_{\text{total}}} \quad (13)$$

Where $NWL_{(t)}$ is the incremental normalized water loss between the initial curing time and time t, W_0 is the initial specimen mass after compaction, W(t) is the specimen mass at the curing time t, and W_{total} is the total water content added to the specimen before compaction, constituted by absorbed water, bitumen emulsion water and added water for compaction. Graziani et al. [23] applied the Michaelis- Menten

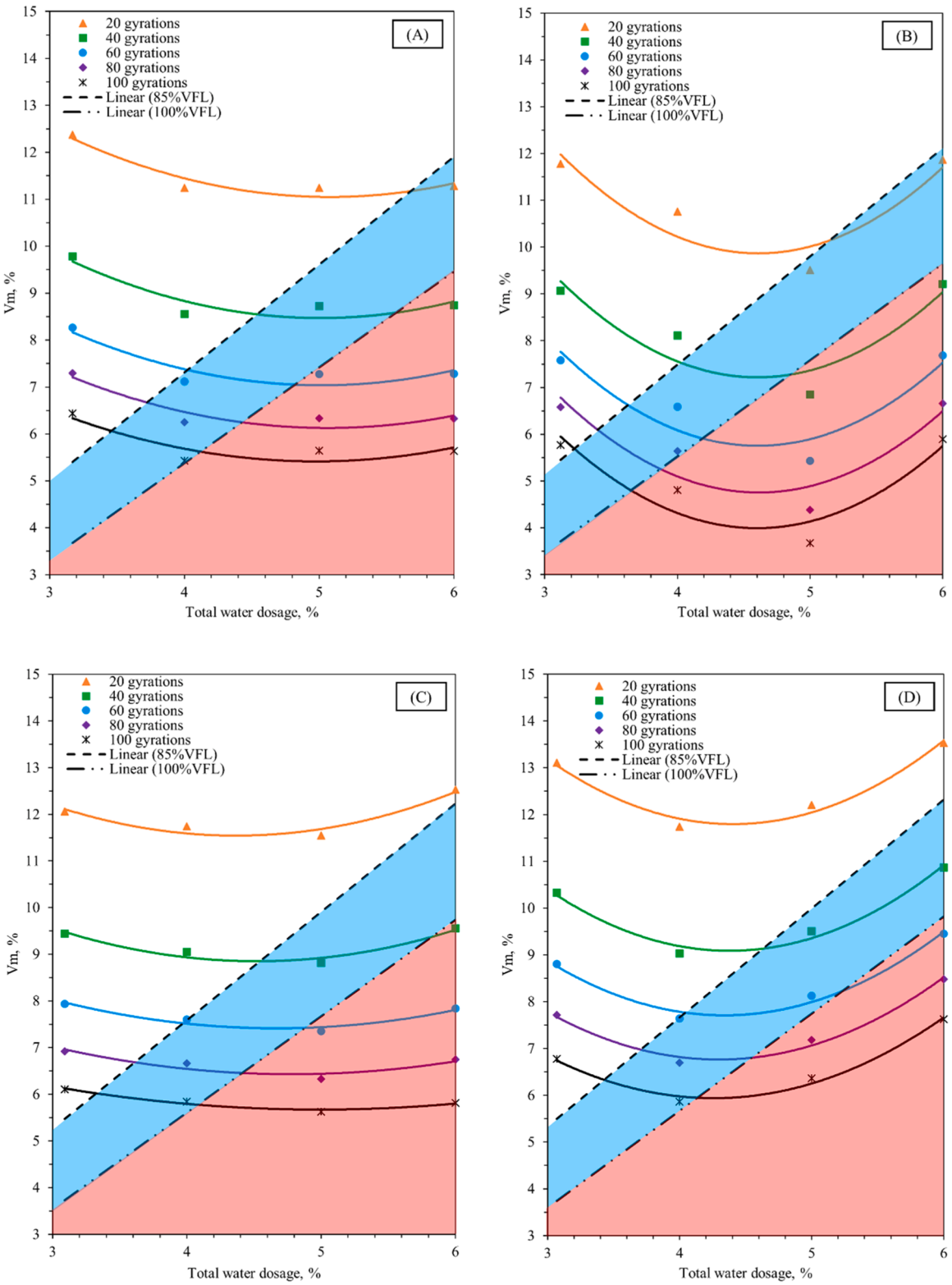

Fig. 10. V_m% as a function of total water dosage for (A): 60LUW, (B): 80LUW, (C): 90LUW, and (D): 100LUW.

(MM) model to model water evaporation over time. The model is a non-linear hyperbolic function which describes an asymptotic evolution of the measured response (evaporation) as a function of time. Eq. (14) shows the Michaelis-Menten model after the first day of curing.

$$y(t) = y_1 + \frac{(y_A - Y_1) \bullet (t-1)}{(H-1) + (t-1)} \quad (14)$$

Where y(t) is water loss, y_A is the asymptotic value, y_1 is associated to -day 1, t is curing days, and H is related to the time it takes for y(t) to get to a value which is in the middle of y_1 and y_A.

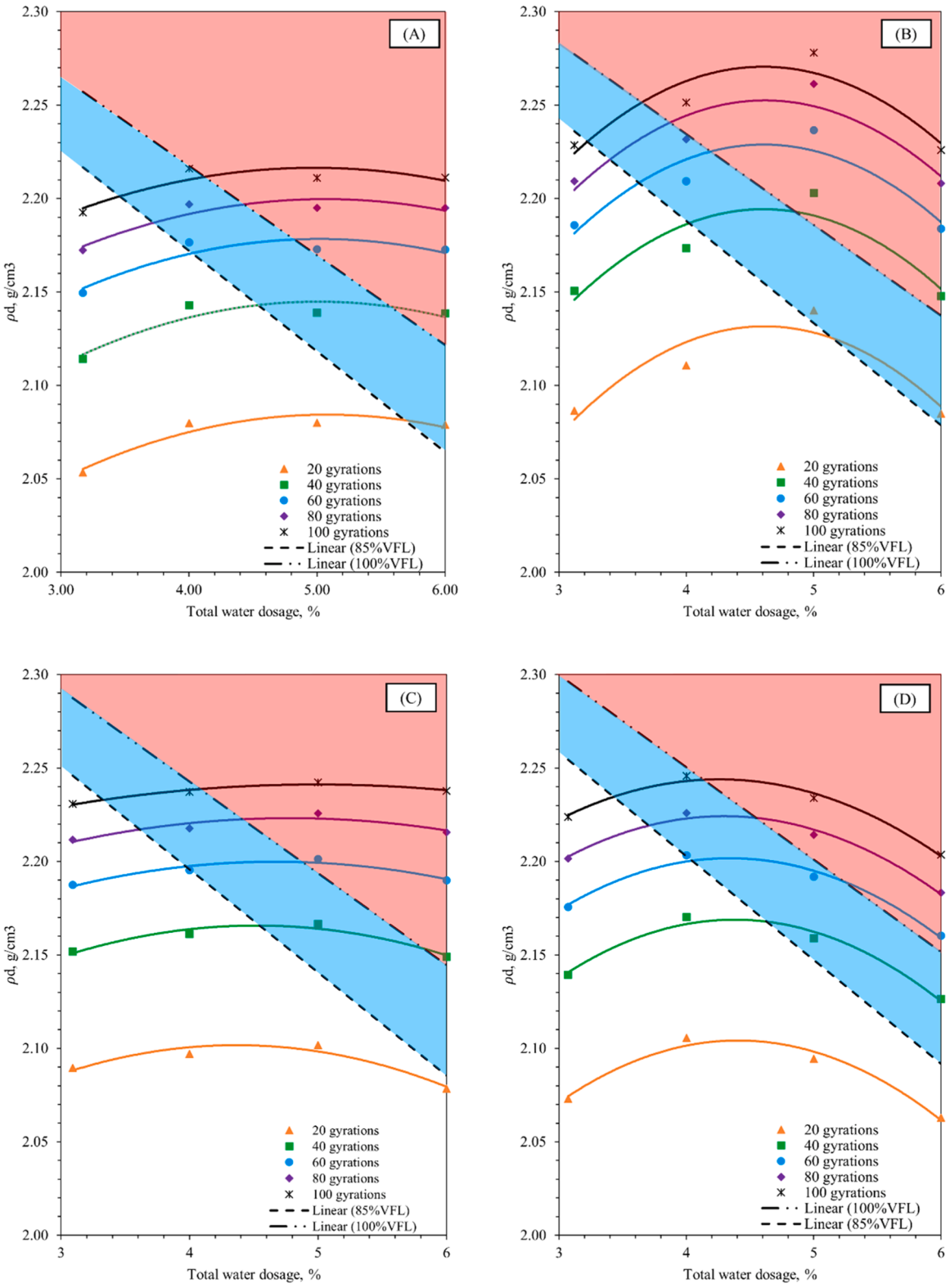

Fig. 11. ρd as a function of total water dosage for (A): 60LUW, (B): 80LUW, (C): 90LUW, and (D): 100LUW.

3.8. Indirect tensile strength (ITS)

The Indirect tensile strength (ITS) of the 60, 80, 90, and 100LUW was determined according to ASTM D6931. The measurements were performed at a loading rate of 51 mm/minute at room temperature. During the test, a compressive load is applied to the cylindrical specimens at a constant rate along a vertical diametric plane to measure the tensile characteristics of the mixtures. The specimens' tensile strength (St) is calculated using Eq. (15).

$$S_t(kPa) = \frac{2000 \quad P}{\pi * t * D} \tag{15}$$

Where P is the maximum load applied in Newton, t is the specimen

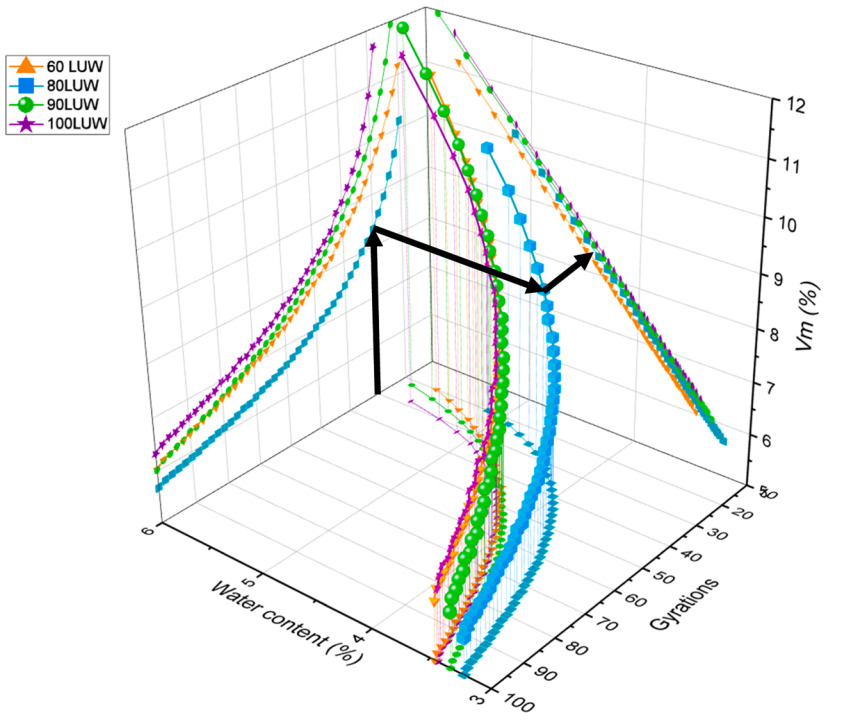

Fig. 12. 3-D graph including the number of gyrations, water content, and V_m% for different mixtures and the selection process of the optimum mixtures.

thickness in mm, and D is the specimen diameter in mm.

4. Results and discussion

4.1. BSM compaction

Fig. 5 illustrates two key volumetric properties of BSM during compaction, namely V_m and VFL, for 60LUW, 80LUW, 90LUW, and 100LUW at moisture contents of 3 %, 4 %, 5 %, and 6 %, as a function of the logarithm of the number of gyrations. Based on the observations, V_m converges, whereas VFL diverges as the compaction level increases from 1 to 100 gyrations. Furthermore, V_m decreases with increasing moisture content up to 5 %, followed by an increase at 6 % water content. In contrast, VFL exhibits consistent growth across the full range of moisture contents. Also, at the end of compaction, V_m for the entire mixture ranges from 3.5 % to 8 %, with the lowest value observed for 80LUW at 5 % water content and the highest for 100LUW at 6 % water content. Similarly, VFL varies between 75 % at the lowest water level in graph (A) and approximately 150 % for 80LUW at 5 % water content in graph (C).

The reduction in V_m with increasing compaction effort results in an increase in VFL as the available space for liquids (water and bitumen emulsion) decreases. The 100LUW mixtures exhibit the lowest VFL and the highest V_m across different moisture contents. Conversely, 80LUW consistently shows the highest VFL and the lowest V_m across various moisture contents.

4.2. Workability and compactability

Fig. 6 illustrates the Workability and compactability of the 60LUW, 80LUW, 90LUW, and 100LUW at different water dosage levels. The figure is divided into four distinct quadrants, including quadrant (A), which shows a lower workability but higher compactability; quadrant (B), which shows a lower workability and lower compactability; quadrant (C), which shows a higher compactability and higher workability; and quadrant (D), which shows the mixtures with lower compactability but higher workability.

To better understand the overall behaviour of the mixtures in terms of workability and compactability at different packing conditions, the centroids for each LUW level were calculated. The centroid represents the average trend of the mixtures, providing a single representative point for the data group. By plotting the centroids, the general shift in the workability and compactability can be visualized, which simplifies the interpretation of the data sets and is calculated using the following formula.

$$(\bar{x}, \quad \bar{y}) = \left(\frac{x_1 + x_2 + \ldots + x_n}{n}, \frac{y_1 + y_2 + \ldots + y_n}{n}\right) \tag{16}$$

Where $\bar{x}$ and $\bar{y}$ represent the centroids for compactability and workability, n represents the number of data points, $x_1 + x_2 + \ldots + x_n$ are the sum of the compactabilities, and $y_1 + y_2 + \ldots + y_n$ are the sum of workabilities.

The centroid for 60LUW exhibits the lowest compactability, while 90LUW shows the highest compactability among the mixtures. As indicated by their void content at 10 gyrations, the centroid for 100LUW mixtures exhibits the lowest workability, while the best workability is associated with 80LUW mixtures. However, the highest compactability among the mixtures is related to 90LUW mixtures. Even though the 80LUW mixtures centroid does not position them the best in compactability, they provide better compactability and moderate workability compared to other mixtures.

4.3. Weight loss due to compaction

Fig. 7 illustrates VFL at the end of compaction (100 gyrations) as a function of water loss. As the water content in the mixtures increases, the water loss due to water squeezing during compaction increases. The mixtures without extra water exhibited a VFL of almost equal to or below 85 %, corresponding to about 0.10 % and less water loss. However, as the water content increased to 4 %, despite the weight loss below 0.8 %, the 60, 80, 90, and 100LUW mixtures experienced liquid seepage from the mould. At the same time, the 80LUW mix and all other mixtures with a total water content of 5 % and 6 % experienced a VFL of 100 % or above, indicating an oversaturation state, as shown in Fig. 8. In

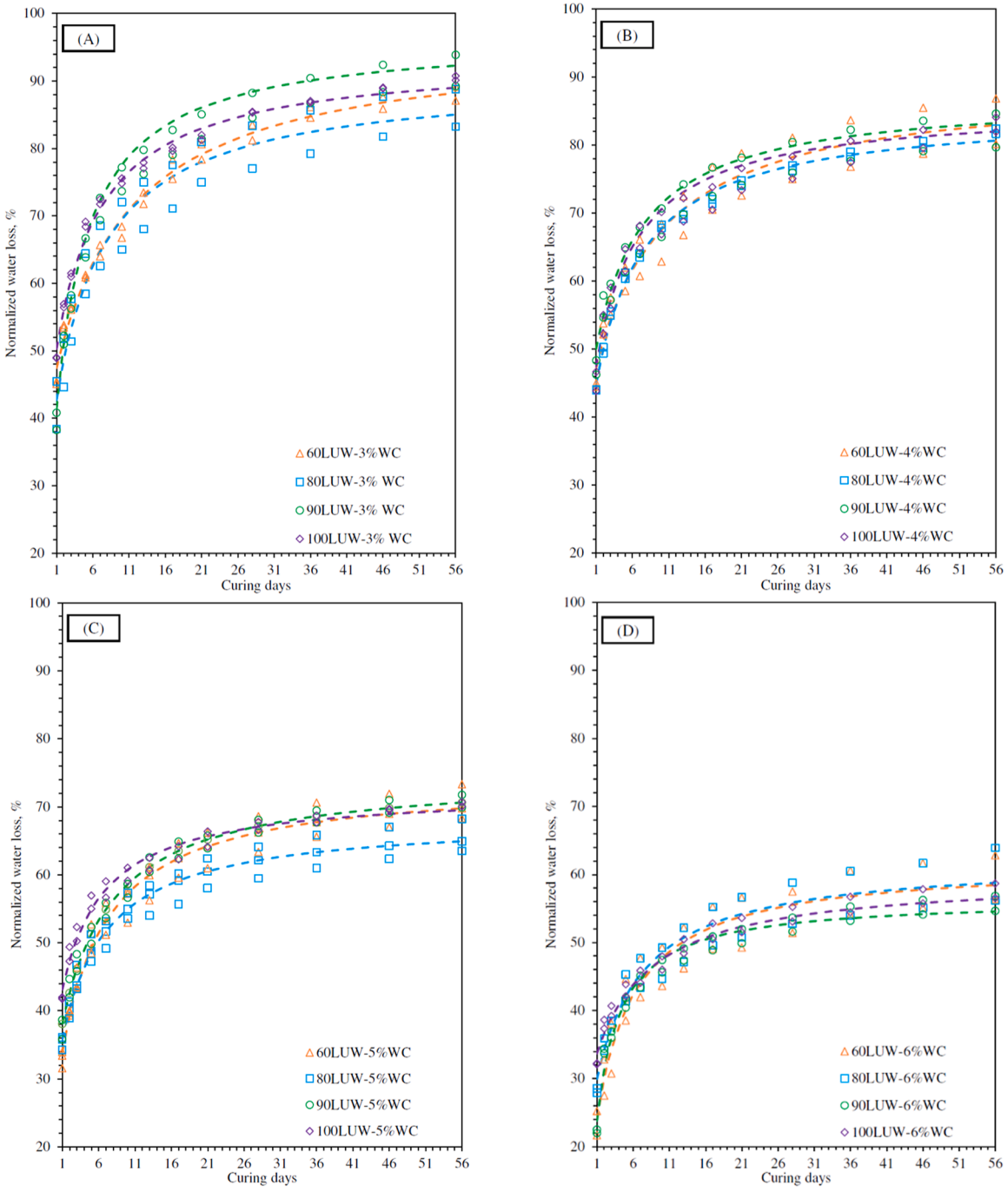

Fig. 13. Normalized evolutive water loss as a function of curing days.

these mixtures, excessive seepage happened due to internal pressure generated by incompressible water and the external compaction pressure exerted by the SGC.

4.4. Volumetric analysis and optimization

Fig. 9 illustrates the variation of VFL as a function of total water content for the four gradations (60LUW, 80LUW, 90LUW, and 100LUW) at five different levels of gyrations (20, 40, 60, 80, and 100 gyrations). In these graphs, The Red area corresponds to a VFL above 100 %, the blue area corresponds to a VFL between 85 % and 100 %, and the white area corresponds to a VFL below 85 %.

It was observed in Section 4.2 of the paper that beyond the 85 % VFL, the liquid, which contains water, some fines, and bitumen emulsion, starts seeping out from the mixtures during compaction [9]. The theoretical VFL values exceeding 100 % indicate that not only are the voids completely saturated at 100 % VFL, but also that excess compaction causes the definite discharge of the liquid, as calculated theoretically. Not surprisingly, an increase in either water content or gyration numbers leads to a higher VFL.

However, as the water content increases, the VFL increases logarithmically, leading to a higher VFL at higher water content levels. Additionally, with the increase in compaction effort, filling the voids with liquid across all gradations requires more effort. This indicates that the mixtures are being saturated, and the additional compaction effort does not significantly change the liquid held in the voids.

It can also be observed that as the gradation changes from 60LUW to 80LUW, the VFL curves exhibit a steeper rise, suggesting that as the

Table 5
Michaelis-Menten model fitting parameters.

Mixture	Y1	YA	H
60LUW–3 % WC	43.10	96.28	10.04
80LUW–3 % WC	42.71	90.46	8.06
90LUW–3 % WC	41.49	96.70	5.77
100LUW–3 % WC	50.30	93.61	7.52
60LUW–4 % WC	47.20	89.20	10.57
80LUW–4 % WC	44.78	85.10	8.97
90LUW–4 % WC	50.02	87.30	7.72
100LUW–4 % WC	47.48	85.70	6.92
60LUW–5 % WC	33.94	74.00	7.49
80LUW–5 % WC	35.83	68.24	7.27
90LUW–5 % WC	38.08	74.84	8.13
100LUW–5 % WC	40.11	68.95	6.76
60LUW–6 % WC	24.02	61.79	6.36
80LUW–6 % WC	29.96	62.26	7.66
90LUW–6 % WC	23.46	55.87	4.59
100LUW–6 % WC	33.72	59.71	8.95

mixture coarseness increases from 60LUW to 80LUW, the mixture is more likely to reach saturation, followed by seepage from the mixture. From 80LUW to 90LUW and subsequently to 100LUW, there is a reduction in saturation sensitivity, followed by a delay in seepage. Since the blue and red regions represent the areas where discharge and confident seepage of liquid occur (because 100 % of the voids are filled with liquid), these areas should be avoided for compaction of the mixtures. Only the white region should be considered.

Fig. 10 and 11 show the effects of different Bailey gradations (60LUW, 80LUW, 90LUW, and 100LUW), total water contents, and the number of gyrations on V_m and dry density. As discussed earlier, the white, blue, and red regions represent VFLs of up to 85 %, 85–100 %, and above 100 %, respectively, with linear trends separating them. The figure demonstrates that generally increasing the total water content by up to 4–5 % caused the V_m to decrease and the dry density to increase at all gyration numbers. With the increase in water content from 4 % to 5 %, the V_m rises, and the dry density reduces again. The V_m reduction and dry density increase were more pronounced for 80LUW and 100LUW. It is also evident that with the increase in the gyration numbers, an expected decrease in V_m and an increase in dry density occur.

Interestingly, as the mixtures become coarser from 60LUW to 80LUW, the materials become more sensitive to moisture content, especially at 4 % and 5 % total water. Also, there is an increase in dry density with the increase in the coarseness up to 80LUW. A reduction in dry density is observed from 80 LUW to 90 and 100 LUW. On the other hand, it can be seen that the dry densities of 90LUW and 100LUW are very close. It can also be observed that as the gyration level increases, the dry density of the mixtures becomes more similar, indicating that the sensitivity of dry density to the gyration level decreases, and the mixtures become denser within the same volume.

The dry density behaviour of the mixtures is highly dependent on the gradation, the moisture content, and the gyrational levels. At a lower number of gyrations of 20, the coarser gradations (90LUW and 100LUW) struggle to reach the same level of dry density before oversaturation compared to the finer gradations (60LUW and 80LUW), especially at higher total water contents. This indicates that mixtures with coarser gradations are more prone to liquid buildup in their voids, which limits their ability to be compacted more effectively. It is more desirable to have a compaction level and water content where the mixtures reach their maximum density before crossing the 85 % VFL line, and the mixtures achieve their optimal compaction before any liquid discharge.

The 3-D graph in Fig. 12 illustrates V_m as a function of water content and the number of gyrations for 60LUW, 80LUW, 90LUW, and 100LUW when the mixtures reach an optimal VFL of 85 %. It is clear that with the increase in gyration numbers at the optimal VFL, V_m experiences a reduction. It can be noted that the mixture's V_m is emerging at the end of compaction. Reference found that 30 gyrations of the SGC represent the field compaction of CIR. Therefore, 30 gyrations were selected to find the water content needed, followed by the V_m generated in the mixtures. It can be seen that among the mixtures, the 80LUW mix exhibits a lower V_m than the other mixtures at VFL of 85 % and at all gyration levels.

4.5. Curing, evolutive water loss, and water loss modelling

Fig. 13 shows the normalized (from 0 % to 100 %) evolution of water loss at 1st, 2nd, 3rd, 5th, 7th, 10th, 13th, 17th, 21st, 28th, 36th, 46th, and 56th days of curing for four types of gradations including 60LUW, 80LUW, 90LUW, and 100LUW and the total water contents of 3 %, 4 %, 5 %, and 6 %. The data were normalized based on the initial weight of the specimen immediately after compaction. As seen in the figure, the evaporation data were modelled using the Michaelis-Menten model. Table 5 presents Y1, YA, H, and R2 of the mixtures.

The effect of initial moisture and gradation on the evaporation behaviour of water in aggregate mixes with various percentages (%) of LUW and water contents was investigated using the Michaelis-Menten model. The results show that specimens with low water levels (3 % and 4 %) exhibit the highest initial evaporation rates (Y1), indicating a rapid release of moisture under these low moisture conditions. This follows the model's asymptotic values (YA), which suggest that these mixtures ultimately give a greater amount of evaporation than mixtures with a higher water content. In particular, finer gradations, such as 60LUW, demonstrate more prolonged evaporation, as evidenced by higher YA values and increased half-times (H). This suggests that finer particulates retain moisture for a more extended period, potentially due to greater surface area interactions or capillary effects. In contrast, coarser gradations, such as 100LUW, exhibit more efficient moisture release, as evidenced by lower asymptotic values and a faster stabilization process (lower H), particularly at elevated initial moisture levels. The significance of particle size distribution and initial water content in determining the evaporation kinetics of these materials is further

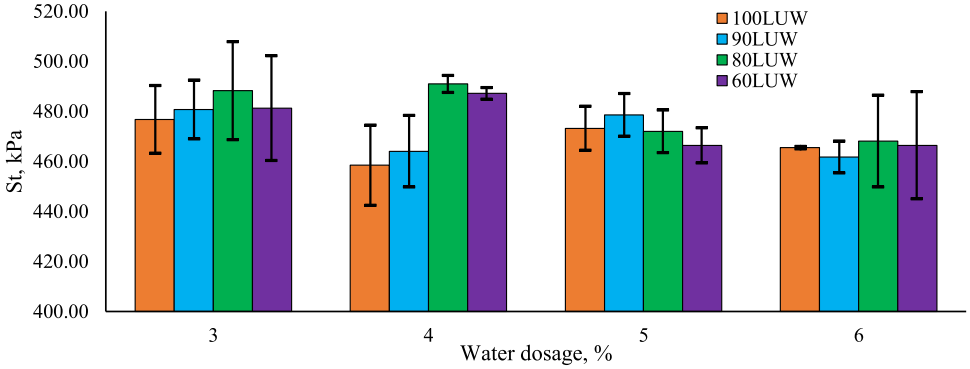

Fig. 14. ITS results after 56 days of curing.

illustrated by this trend. Also, the highest variability of water loss is for the water content of 3 %, shown in graph "A", and since no water was discharged from these mixtures during compaction (seen in the previous section with VFL of 85 % and below), it could suggest how the mixtures response to evaporation when they are not completely saturated. With one of the highest water losses due to compaction at an initial water content of 3 %, the 80LUW mixture exhibits the lowest water evaporation compared to the other mixtures. However, at the highest level of water content (6 % water content), the 90LUW mix, which had relatively higher average water loss due to compaction, showed the lowest water loss due to evaporation.

It is also clear from the modelled evaporation using the Michaelis-Menten model that as the water content increases, the evaporation on the first day (Y1) changes from 90LUW at 3 % to 80LUW at 4 % and 60LUW at 5 %, and then again to 90LUW at 6 % water content. 100LUW had the highest water evaporation on the first day, except at 4 % water content, whereas 60LUW and 80LUW showed slightly higher evaporation.

4.6. Indirect tensile strength

Fig. 14 shows the ITS results for 60, 80, 90, and 100LUW at water contents ranging from 3 % to 6 %, compacted to 100 gyrations and cured for 56 days at ambient temperature and humidity. The results indicate that 80LUW mixtures perform better than the rest at water contents of 3 %, 4 %, and 6 %. Meanwhile, at 5 % water content, 90LUW showed higher tensile strength. Yet, the highest tensile strength, related to 80LUW, is approximately 490 kPa and remains similar at water contents of 3 % and 4 %. The lowest ITS is approximately 460 kPa, related to 100LUW, at a water content of 4 %.

5. Conclusion

This research studied the volumetric optimization of bitumen-stabilized materials (BSM) by integrating the Bailey packing method with an upper limit on voids filled with liquid (VFL). Mixtures with four different loose unit weight (LUW) gradations, including 60, 80, 90, and 100LUW, were produced using the Bailey method, with water contents ranging from 3 % to 6 %. The specimens were compacted up to 100 gyrations using SGC, followed by curing under controlled environmental conditions. The volumetric analysis of the mixes during compaction, water loss at the end of compaction, and evolutive water evaporation of the specimens after compaction were measured up to 56 days.The study suggests that employing the Bailey method and limiting the VFL can be effective in volumetric analysis, as well as in optimizing compaction properties such as workability and compactability, and in the BSM. This demonstrates the potential for sustainable pavement solutions that use 100 % reclaimed asphalt.

(1) The centroid for workability and compactability of the mixtures shows diverse behaviour. The study shows that in the range of experimented loose unit weight, 80LUW produces improved workability and compactability. As the material becomes finer (60LUW), both workability and compactability worsen. In contrast, as the gradation becomes coarser (90LUW and 100LUW), compactability is maintained almost unchanged, but workability is reduced.
(2) The observations showed that for a given mixture, the water loss at the end of compaction could be used to estimate the suitable total water content without experiencing leakage.
(3) The results indicate that the reduction and increase of V_m with the increase in percent (%) LUW follows the Bailey method approach and that the Bailey method effectively identifies the mixture with the highest packing density for BSM.
(4) The study identified that a mixture produced using gradation corresponding to 80LUW and compacted at approximately 4–4.5 % of total water content minimized the V_m (combined air and intergranular water content), preventing liquid seepage while achieving a higher post-curing strength. In contrast, coarser blends of 90LUW and 100LUW required higher water content to achieve densification and tended to lose strength when excessive saturation occurred. Based on the observations, a threshold of VFL $\leq$ 85 can be used as a practical criterion for BSM production.

It is recommended that future research focus on diverse sources of RAP and curing conditions, as well as the freeze-thaw cycles effect on void properties, and relate the proposed volumetric targets to long-term performance metrics.

CRediT authorship contribution statement

Sajjad Noura: Writing – review & editing, Writing – original draft, Visualization, Methodology, Investigation, Formal analysis, Conceptualization. **Andrea Graziani:** Writing – review & editing, Validation, Supervision, Methodology, Investigation, Formal analysis, Conceptualization. **Alan Carter:** Writing – review & editing, Validation, Supervision, Project administration, Methodology, Investigation, Formal analysis, Conceptualization.

Declaration of Competing Interest

The authors declare that they have no known competing financial interests or personal relationships that could be perceived to influence the work reported in this paper.

Data availability

Data will be made available on request.

References

[1] F. Xiao, S. Yao, J. Wang, X. Li, S. Amirkhanian, A literature review on cold recycling technology of asphalt pavement, Constr. Build. Mater. 180 (2018) 579–604, https://doi.org/10.1016/j.conbuildmat.2018.06.006.
[2] S. Salehi, M. Arashpour, J. Kodikara, R. Guppy, Sustainable pavement construction: a systematic literature review of environmental and economic analysis of recycled materials, J. Clean. Prod. 313 (2021) 127936, https://doi.org/10.1016/J.JCLEPRO.2021.127936.
[3] P. Orosa, A.R. Pasandín, I. Pérez, Compaction and volumetric analysis of cold in-place recycled asphalt mixtures prepared using gyratory, static, and impact procedures, Constr. Build. Mater. 296 (2021) 123620.
[4] S. Raschia, D. Perraton, A. Graziani, A. Carter, Influence of low production temperatures on compactability and mechanical properties of cold recycled mixtures, Constr. Build. Mater. 232 (2020), https://doi.org/10.1016/j.conbuildmat.2019.117169.
[5] C.W. Schwartz, B.K. Diefenderfer, B.F. Bowers, Material properties of cold in-place recycled and full-depth reclamation asphalt concrete, 2017.
[6] C. Zhu, H. Zhang, Q. Li, Z. Wang, D. Jin, Influence of different aged RAPs on the long-term performance of emulsified asphalt cold recycled mixture, Constr. Build. Mater. 458 (2025) 139680.
[7] M. Meocci, A. Grilli, F. La Torre, M. Bocci, Evaluation of mechanical performance of cement–bitumen-treated materials through laboratory and in-situ testing, Road. Mater. Pavement Des. 18 (2017) 376–389.
[8] R. Kumar, A. BR, A.K. Chandrappa, S. Swaroopa Kar, U.C. Sahoo, Bitumen stabilised materials for sustainable pavements: a review, Road. Mater. Pavement Des. (2024) 1–33.
[9] H. Du, R. Li, H. Zhu, P. Qi, L. Lei, S. Yang, Q. Tan, Y. Xu, Y. Yang, Evolutive properties of emulsified asphalt cold recycled mixtures at early stage, Constr. Build. Mater. 456 (2024) 139320.
[10] Y. Yao, G. Xu, M. Wu, M. Zhao, Exploring the influence of cement and cement hydration products on strength and interfacial adhesion in emulsified cold recycled mixture: a molecular dynamics and experimental investigation, Constr. Build. Mater. 409 (2023) 134050.
[11] L.P. Thives, E. Ghisi, Asphalt mixtures emission and energy consumption: a review, Renew. Sustain. Energy Rev. 72 (2017) 473–484.
[12] R. Mariyappan, J.S. Palammal, S. Balu, Sustainable use of reclaimed asphalt pavement (RAP) in pavement applications—a review, Environ. Sci. Pollut. Res. 30 (2023), https://doi.org/10.1007/s11356-023-25847-3.
[13] C. Mignini, F. Cardone, A. Graziani, Complex modulus of cement-bitumen treated materials produced with different reclaimed asphalt gradations, Mater. Struct. /Mater. Et. Constr. 55 (2022), https://doi.org/10.1617/s11527-022-02009-4.

[14] P. Orosa, I. Pérez, A.R. Pasandín, Evaluation of the shear and permanent deformation properties of cold in-place recycled mixtures with bitumen emulsion using triaxial tests, Constr. Build. Mater. 328 (2022), https://doi.org/10.1016/j.conbuildmat.2022.127054.
[15] A. Academy, Interim technical guidelines (TG2): The design and use of foamed bitumen treated materials, (2020).
[16] V.T. Thushara, A. Behera, J.M. Krishnan, Investigating permanent deformation of bituminous mixtures designed using particle-packing based gradation and mastic optimization, Mater. Struct. 58 (2025) 1–20.
[17] S. Badeli, A. Carter, G. Doré, The importance of asphalt mixture air voids on the damage evolution during freeze-thaw cycles, Can. Tech. Asph. Assoc. (2016) 13–16.
[18] B. Lira, Influence of aggregates on permanent deformation of asphalt, Elektroniskt) Tillgänglig: Influence of Aggregates (2023-08-17) (2020).
[19] O. Xu, Z. Wang, R. Wang, Effects of aggregate gradations and binder contents on engineering properties of cement emulsified asphalt mixtures, Constr. Build. Mater. 135 (2017), https://doi.org/10.1016/j.conbuildmat.2016.12.095.
[20] S. Raschia, C. Mignini, A. Graziani, A. Carter, D. Perraton, M. Vaillancourt, Effect of gradation on volumetric and mechanical properties of cold recycled mixtures (CRM), (2019). https://doi.org/10.1080/14680629.2019.1633754.
[21] Z. Liu, L. Sun, A review of effect of compaction methods on cold recycling asphalt mixtures, Constr. Build. Mater. 401 (2023) 132758.
[22] S. Noura, R. Ajmi, M. Mihajlovic, A. Carter, Characterization of cold recycled asphalt mixes with indirect tensile strength and complex modulus. International Symposium on Asphalt Pavement & Environment, Springer, 2024, pp. 759–763.
[23] S.N.A. Aker, H. Ozer, Aggregate packing characterisation of cold recycled mixtures, Int. J. Pavement Eng. (2022), https://doi.org/10.1080/10298436.2022.2078977.
[24] A. Grilli, A. Graziani, E. Bocci, M. Bocci, Volumetric properties and influence of water content on the compactability of cold recycled mixtures, Mater. Struct. /Mater. Et. Constr. 49 (2016), https://doi.org/10.1617/s11527-016-0792-x.
[25] W.R. Vavrik, W.J. Pine, S.H. Carpenter, Aggregate blending for asphalt mix design Bailey method, Transp. Res. Rec. (2002), https://doi.org/10.3141/1789-16.
[26] G. Flores, J. Gallego, L. Miranda, J.R. Marcobal, Design methodology for in situ cold recycled mixtures with emulsion and 100% rap, Constr. Build. Mater. 216 (2019) 496–505.
[27] Z. Liu, L. Sun, J. Zhai, W. Huang, A review of design methods for cold in-place recycling asphalt mixtures: design processes, key parameters, and evaluation, J. Clean. Prod. 370 (2022) 133530.
[28] C. Zhu, H. Zhang, L. Huang, C. Wei, Long-term performance and microstructure of asphalt emulsion cold recycled mixture with different gradations, J. Clean. Prod. 215 (2019), https://doi.org/10.1016/j.jclepro.2019.01.103.
[29] C. Zhu, H. Zhang, H. Guo, C. Wu, C. Wei, Effect of gradations on the final and long-term performance of asphalt emulsion cold recycled mixture, J. Clean. Prod. 217 (2019), https://doi.org/10.1016/j.jclepro.2019.01.264.
[30] S. Raschia, T.B. Moghaddam, D. Perraton, H. Baaj, A. Carter, A. Graziani, Effect of rap source on compactability and behavior of cold-recycled mixtures in the small strain domain, J. Mater. Civ. Eng. 33 (2021) 04021030.
[31] S.S. Dash, M. Panda, Effect of aggregate gradation on cold bituminous mix performance, Adv. Civ. Eng. Mater. 4 (2015), https://doi.org/10.1520/ACEM20140047.
[32] Z. Han, L. Liu, L. Sun, Gradation control method of cold-recycled mixture considering influence of fractal dimensions and false aggregates, Tongji Daxue Xuebao/J. Tongji Univ. 51 (2023), https://doi.org/10.11908/j.issn.0253-374x.22024.
[33] A. Ghavibazoo, M.I.E. Attia, P. Soltis, H. Ajideh, Effect of gradation and aged binder content of reclaimed asphalt pavement (RAP) on properties of cold-recycled asphalt mix, Airfield Highw. Pavements 2017 (2017) 79–89.
[34] H. Yao, L. Li, H. Xie, H.-C. Dan, X.-L. Yang, Gradation and performance research of cold recycled mixture, Road. Pavement Mater. Charact. Model. Maint. (2011) 1–9.
[35] A. Graziani, G. Ferrotti, E. Pasquini, F. Canestrari, An application to the European practice of the Bailey method for HMA aggregate grading design, ProcediaSoc. Behav. Sci. 53 (2012) 990–999.